PHYSICAL REVIEW B **80**, 180408(R) (2009)

# Anomalous induction of ferroelectric polarization by magnetization reversal in the phase-separated multiferroic manganite $Eu_{0.8}Y_{0.2}MnO_3$

S. Danjoh, J.-S. Jung, H. Nakamura, Y. Wakabayashi, and T. Kimura
*Division of Materials Physics, Graduate School of Engineering Science, Osaka University, Toyonaka, Osaka 560-8531, Japan*
(Received 1 October 2009; published 10 November 2009)

Regarding electronic phase separation and its magnetoelectric control in multiferroics, we have investigated magnetic and ferroelectric properties of $Eu_{0.8}Y_{0.2}MnO_3$ located near the boundary between a ferromagnetic phase and a ferroelectric phase. We observed special coexistence of the two phases, which fractions are tuned at an arbitrary level by changing the cooling magnetic-field strength. In addition, repeated magnetization reversals by applying an alternating magnetic field induce anomalous enhancement of ferroelectric polarization, suggesting the development of the ferroelectric phase during the magnetization reversal process.

DOI: 10.1103/PhysRevB.80.180408 PACS number(s): 75.80.+q, 61.05.cp, 75.30.Kz, 77.80.Dj

Systems with multiple competing interactions (e.g., relaxor ferroelectrics,[1] colossal magnetoresistive manganites,[2] and frustrated spin systems[3]) often show remarkably complex states of matter as well as rich electronic phase diagrams. In such systems, local inhomogeneity of the electronic structure and/or electronic phase-separation tendencies frequently play crucial roles in their electronic properties and cause extraordinarily gigantic electronic responses.[1–4] Recently, the magnetoelectric (ME) effect, that is, the induction of the electric polarization (magnetization) by external magnetic (electric) fields, has been of renewed interest.[5,6] One of the triggers for such revivals is a recent discovery of a large ME effect in a perovskite-type rare-earth manganite $TbMnO_3$.[7] In $TbMnO_3$, ferroelectricity is induced by a spiral-antiferromagnetic (AFM) order, which breaks inversion symmetry.[8–10] The ionic radius ($r_R$) of $Tb^{3+}$ ion in $TbMnO_3$ is appropriate to bring about the spiral-AFM structures arising from the competing exchange interactions.[11,12] When $Tb^{3+}$ is replaced with other rare-earth ions having larger $r_R$, such as Gd and Eu, the balance of the competition is modified mainly due to the change in Mn-O-Mn bond angle $\phi$.[13] As a result, the spiral-AFM and ferroelectric (SAFM-FE) phase transform into a weakly ferromagnetic and paraelectric (WFM-PE) phase. When $r_R$ (or $\phi$) is appropriate to locate the system on the boundary between the two phases, we can expect local inhomogeneity and/or phase-separation tendency that play some role in the electronic properties and produce unusual electronic responses.

In this Rapid Communication, we report on phase separation and unusual magnetoelectric responses in a multiferroic manganite $Eu_{0.8}Y_{0.2}MnO_3$, which resides on the boundary between the two competing phases. We briefly review earlier results[14,15] for the magnetic and electric phase diagrams of $Eu_{1-x}Y_xMnO_3$ with the *Pbnm* orthorhombic structure. As displayed in Fig. 1(d), $EuMnO_3$ with relatively large $r_R$ of $Eu^{3+}$ shows a canted A-type AFM order with a weak ferromagnetic moment along the *c* axis below 42 K but does not show ferroelectricity (i.e., WFM-PE state).[13,16] By the isovalent doping of $Eu^{3+}$ site with $Y^{3+}$, having smaller $r_R$, the WFM-PE state disappears while the SAFM-FE state with spontaneous polarization along the *a* axis emerges at $x > \sim 0.25$.[17] At the doping level of $x \sim 0.2$, the WFM-PE and the SAFM-FE states keenly compete with each other. An early report[14] suggested the coexistence of ferromagnetism and ferroelectricity in the same phase for $x \sim 0.2$ samples. However, more recent results[15,18] do not support the simul-

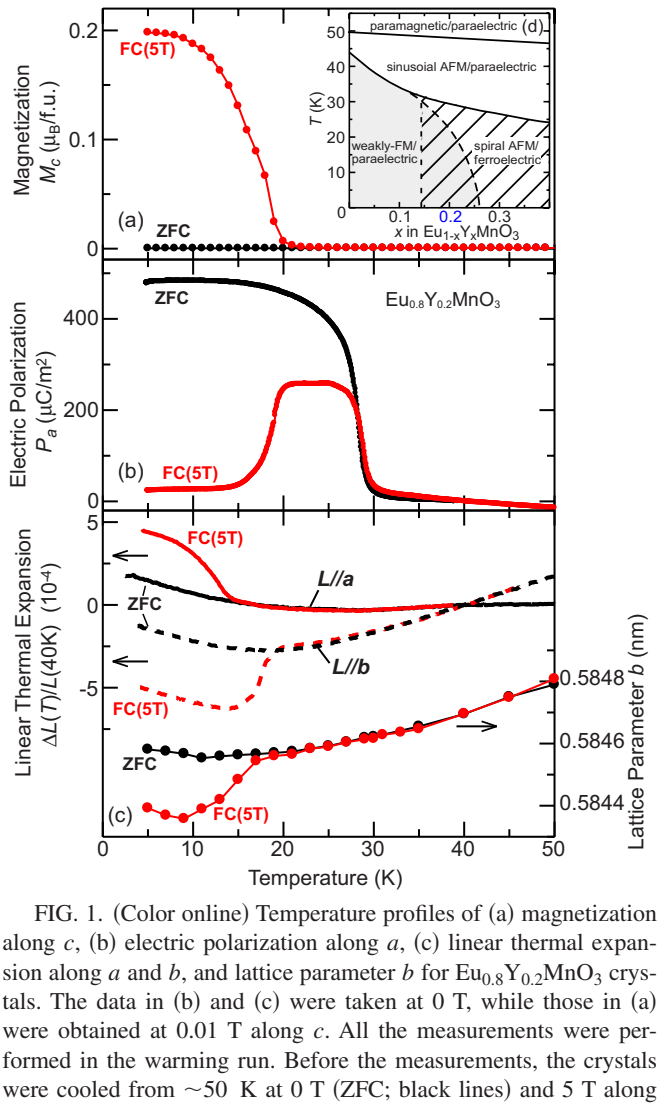


FIG. 1. (Color online) Temperature profiles of (a) magnetization along *c*, (b) electric polarization along *a*, (c) linear thermal expansion along *a* and *b*, and lattice parameter *b* for $Eu_{0.8}Y_{0.2}MnO_3$ crystals. The data in (b) and (c) were taken at 0 T, while those in (a) were obtained at 0.01 T along *c*. All the measurements were performed in the warming run. Before the measurements, the crystals were cooled from ~50 K at 0 T (ZFC; black lines) and 5 T along *c* [FC5T; red lines (gray lines in print)]. (d) Magnetic and electric phase diagrams of $Eu_{1-x}Y_xMnO_3$ (reproduced from Refs. 14 and 15).

 ©2009 The American Physical Society

taneous coexistence. To settle this discrepancy, we investigate magnetic and electric properties in various conditions for $Eu_{0.8}Y_{0.2}MnO_3$, which resides on the boundary between the WFM-PE and the SAFM-FE phases. We found anomalous induction of ferroelectric polarization by applying an alternating magnetic field. The results are discussed in terms of spatial coexistence and competition of ferromagnetic and ferroelectric phases.

Single crystals of $Eu_{0.8}Y_{0.2}MnO_3$ were grown by the floating-zone method. Powder x-ray diffraction (XRD) measurements confirmed the *Pbnm* orthorhombic structure at room temperature. The crystals were oriented using Laue XRD patterns and cut into thin plates with the widest faces normal to the *a* axis. Silver electrodes were then vacuum deposited onto those faces for measurements of the electric polarization along the *a* axis ($P_a$). We made the following measurements in various cooling magnetic-field ($B_{cool}$) conditions. The magnetization along the *c* axis ($M_c$) was measured with a commercial magnetometer. The temperature ($T$) and magnetic-field ($B$) profiles of $P_a$ were obtained by measurements of pyroelectric and magnetoelectric currents, after poling the crystals at ~0.3 MV/m. The linear thermal expansion $\Delta L(T)/L$ parallel to *a* and *b* was measured using a uniaxial strain gauge. Single-crystal XRD measurements using synchrotron x-rays with photon energy of 12 keV were performed at BL-3A equipped with a superconducting magnet in the Photon Factory (KEK).

We first investigated history dependence of magnetic, electric, and structural properties (Fig. 1). Before the measurements, crystals were cooled from ~50 K (above magnetic ordering $T$) to 5 K at $B=0$ T [zero-field cooling (ZFC)] and 5 T [field cooling at 5 T (FC5T)]. Figure 1(a) displays $M_c$-$T$ data (black and red lines) measured in a weak magnetic field (0.01 T), which is applied at 5 K after the above cooling procedures. The ZFC data show no distinct feature in the $M_c$-$T$ curve, while the FC5T data exhibit a steep increase in $M_c$ at $T=20$ K toward lower temperatures. This suggests that only the FC5T procedure makes the system weakly ferromagnetic below 20 K. Such history-dependent feature can also be seen in $P_a$-$T$ curves, as shown in Fig. 1(b). Spontaneous polarization develops below 30 K for both ZFC and FC5T data, meaning that the system becomes ferroelectric. However, only in the FC5T data, the spontaneous polarization almost vanishes again below 20 K, where the weakly ferromagnetic feature arises. These results demonstrate a clear anticorrelation between the (weak) ferromagnetism and ferroelectricity and a history-dependent apparent ground state, i.e., the SAFM-FE state after the zero-field cooling and the WFM-PE state after the field cooling.

A comparison of $\Delta L(T)/L$ data shown in Fig. 1(c) with those of $M_c$ and $P_a$ reveals a magnetostrictive coupling in $Eu_{0.8}Y_{0.2}MnO_3$. Whereas no anomaly in $\Delta L(T)/L$ was observed in the ZFC data,[19] striking changes were observed in the FC5T data at 20 K, where the weakly ferromagnetic moment develops. The $\Delta L(T)/L$ parallel to *a* shows a steeply increase while that along *b* decreases at 20 K toward lower temperatures. Such magnetostrictive features were well reproduced in the change in lattice parameter *b* measured by the XRD measurement, as seen in Fig. 1(c). Thus, as the system undergoes ferromagnetic order, the *a* axis elongates

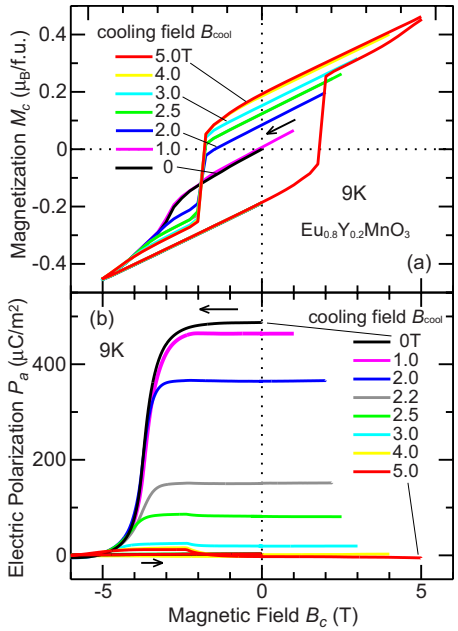


FIG. 2. (Color online) (a) Magnetization along *c* and (b) electric polarization along *a* for $Eu_{0.8}Y_{0.2}MnO_3$ crystals as a function of $B$ parallel to *c* at 9 K. The measurements were done once cooling magnetic fields $B_{cool}$ were applied at ~50 K and the crystals were cooled to 9 K in the respective cooling fields.

while the *b* axis shrinks through the magnetostrictive coupling. The difference in the *b* axis length between the WFM-PE and the SAFM-FE phases will be used to detect the coexistence of the two phases.

To further examine the history-dependent magnetic and electric properties, the cooling-field dependencies of $M_c$ and $P_a$ were measured at a fixed $T$(=9 K). Right before these measurements, the crystal was slowly cooled from ~50 to 9 K at selected cooling fields ($B_{cool}$). As shown in Fig. 2(a), virgin magnetization data for $B_{cool} \leq 1$ T show nearly straight line through the origin at $B > -2.5$ T, suggesting that the system is AFM in the virgin state. By sweeping $B$ down to ~−3 T, a metamagnetic transition occurs. For the virgin curves of $B_{cool} \geq 2$ T, remanent magnetization $M_{rem}$ becomes finite. With increasing $B_{cool}$, the virgin lines shift in parallel toward higher magnetization and $M_{rem}$ steadily increases with increasing $B_{cool}$ up to ~4 T. At $B_{cool} \geq 4$ T, no further increase in $M_{rem}$ was observed. Once the crystal was exposed to $|B|=5$ T, all the magnetization data fall into identical hysteresis curves with coercive field of ~2 T and $M_{rem}$ of $\sim 0.2\mu_B$/f.u. along *c*. The value of $M_{rem}$ is comparable with those in $EuMnO_3$ and $LaMnO_3$, showing the canted A-type AFM order in which the origin of spin canting has been discussed in terms of the single-ion spin anisotropy and the Dzyaloshinskii-Moriya interaction.[20,21] As seen in Fig. 2(b), virgin curves of $P$-$B$ data[22] also depend on $B_{cool}$. With increasing $B_{cool}$, remanent polarization $P_{rem}$ in the virgin curves is suppressed drastically and finally becomes zero at $B_{cool} \geq 4$ T. Once $|B| > 5$ T is applied, $P_a$ almost vanishes in all the $B_{cool}$ data.

It is possible to understand the observed history-dependent magnetic and electric properties in terms of the

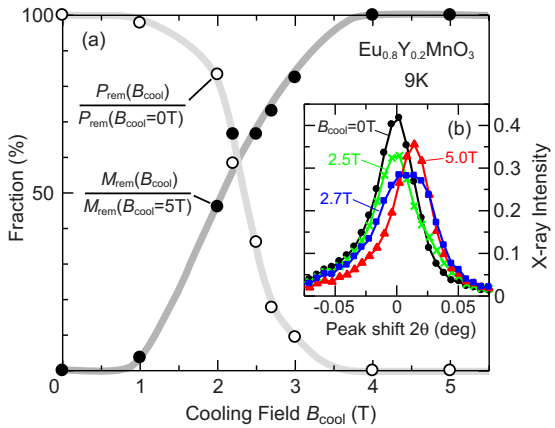


FIG. 3. (Color online) Fractions of the WFM-PE phase (solid circles) and the SAFM-FE phase (open circles) at 9 K as a function of cooling magnetic field for $Eu_{0.8}Y_{0.2}MnO_3$. The fractions were estimated from remanent magnetization and electric polarization in virgin curves. Grey lines are guides for the eyes. (b) Single-crystal x-ray diffraction profiles around the (060) Bragg reflection. The measurements were performed at 9 K and 0 T after the crystal was cooled from ~50 K to 9 K in the respective cooling fields.

coexistence of the WFM-PE and the SAFM-FE phases, which can transform into each other. The systematic evolution of $M_{rem}$ and $P_{rem}$ with increasing $B_{cool}$ can be attributed to the increase in the fraction of the WFM-PE phase at the expense of the SAFM-FE phase volume. Figure 3(a) displays the cooling-field dependence of $M_{rem}(B_{cool})/M_{rem}(B_{cool}=5\ T)$ and $P_{rem}(B_{cool})/P_{rem}(B_{cool}=0\ T)$ for the virgin curves, i.e., the fractions of the WFM-PE and the SAFM-FE phases, respectively. The result suggests that the two phases coexist by cooling the crystal in the intermediate field range of $1\ T<B_{cool}<4\ T$.

The single-crystal XRD measurements confirmed the coexistence of different phases for the intermediate $B_{cool}$ region. Figure 3(b) displays XRD profiles around the (060) Bragg reflection measured at 0 T and 9 K. Before the respective measurements, the crystal was first cooled from ~50 to 9 K at selected $B_{cool}$ and then $B_{cool}$ was removed at 9 K. The diffraction pattern of $B_{cool}=5\ T$ shows explicit shift in the peak position toward higher $2\theta$ with respect to that of $B_{cool}=0\ T$, indicating a decrease in the $b$ axis length after the field cooling procedure with $B_{cool}=5\ T$ [see also Fig. 1(c)]. No peak broadening was observed in both the $B_{cool}=0$ and 5 T data, while those of $2\ T<B_{cool}<3\ T$ show noticeable broadenings, demonstrating the coexistence of two phases with different $b$ axis lengths in the intermediate $B_{cool}$ data. Considering the magnetostrictive coupling presented in Fig. 1, these two phases should correspond to the WFM-PE and the SAFM-FE phases.

The phase-separated multiferroic manganite exhibits anomalous induction of ferroelectric polarization by applying an alternating magnetic field. Figures 4(a) and 4(b) show $M_c$ and $P_a$ as a function of $B$ at 9 K, respectively. Before both the measurements, at first, magnetic fields were applied ($B_{start}=+5\ T$ and $+8\ T$ for measurements of $M_c$ and $P_a$, respectively) and were swept down to $-B_{start}$ (i to ii in Fig. 4).

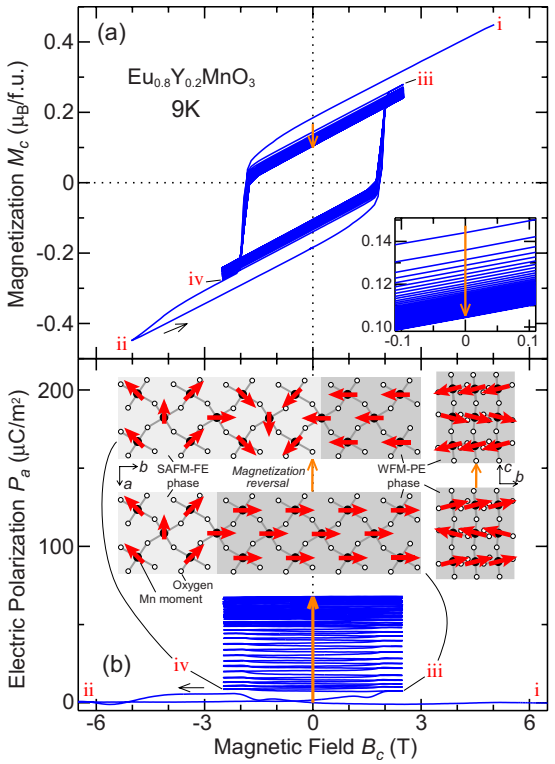


FIG. 4. (Color online) (a) Suppression of magnetization and (b) promotion of electric polarization by applying an alternating magnetic field for $Eu_{0.8}Y_{0.2}MnO_3$. Orange arrows denote the evolution of magnetization or electric polarization. The inset of (a) shows a magnified view of the magnetization curves. Roman numerals denote the order of measurements. Insets of (b): schematic drawings of spin configurations near the boundary between the SAFM-FE and the WFM-PE phases and a possible evolution of the SAFM-FE phase during the magnetization reversal process.

In the course of sweeping $B$ to $-B_{start}$, the magnetization reversal and the metamagnetic transition occur at around $-2$ T and $-4$ T, respectively [Figs. 2(a) and 4(a)]. The magnetic anomalies accompany electric ones. Although no finite polarization is observed at $B_{start}$, $P_a$ starts to develop at around $-2$ T and becomes nearly constant at $-2.5\ T>B>-4\ T$. With further decreasing $B$, $P_a$ starts to decrease at ~$-4$ T and vanishes again at ~$-6$ T. After sweeping $B$ down to $-B_{start}$, we set $B$ to $B_{cycle}=+2.5\ T$ (ii to iii in Fig. 4). Magnetization and polarization curves during this procedure also show the magnetization reversal and the development of $P_a$ at around 2 T, and then we swept $B$ between $+B_{cycle}$ and $-B_{cycle}$ (between iii and iv in Fig. 4), repeatedly, that is, applied a low frequency alternating $B$. As indicated by an orange arrow in Fig. 4(a), the more $B$ was swept between $\pm B_{cycle}$, the smaller magnetization becomes. In accordance with the suppression of $M_c$, surprisingly, $P_a$ steadily increases with increasing the number of cycle for $B$ scan, as indicated by an orange arrow in Fig. 4(b).

We speculate that the anomalous increase in $P_a$ by applying an alternating $B$ is related to the increase in volume and/or number of the SAFM-FE phase. In the lower insets of Fig. 4(b), we illustrate a possible change in spin configuration near the boundary between the SAFM-FE and the

WFM-PE regions during the process of magnetization reversal. Whenever the system undergoes the magnetization reversal, the WFM-PE region at the edge of the boundary can transform into the SAFM-FE state, as illustrated in the inset of Fig. 4(b). In addition, the magnetization reversal may occasionally yield additional magnetic domains for the WFM-PE region as well as accompanied domain walls. In general, magnetic moments in domain walls of ferromagnetic materials gradually rotate from the direction in one domain to the other. Especially, in a Néel domain wall, where magnetic moments rotate in the plane, its spin configuration can be viewed as a portion of that in the SAFM-FE phase with the spin spiral plane normal to $c$.[13] Thus, it is possible that the magnetic domain walls act as nuclei of the SAFM-FE phases. Note that the induction of electric polarization by Néel domain walls has been pointed out in terms of the symmetry-based discussion.[9]

In summary, we investigated magnetic and ferroelectric properties in $Eu_{0.8}Y_{0.2}MnO_3$ located near the boundary between a weakly ferromagnetic and paraelectric phase and a spiral-antiferromagnetic and ferroelectric phase. We found that the magnitude of magnetization and electric polarization can be tuned to a considerable extent by magnetic-field history, which is ascribed to spatial coexistence of the two phases transforming into each other. The unique simultaneous control of ferromagnetism and ferroelectricity can be achieved in phase-separated multiferroics, in which ferromagnetic and ferroelectric phases are nearly degenerated.

We thank Y. Sekio and K. Kimura for help with experiments and enlightening discussions. This work was supported by KAKENHI (Grants No. 20674005, No. 20001004, and No. 19052001) and Global COE Program (G10).

[1] A. A. Bokov and Z.-G. Ye, J. Mater. Sci. **41**, 31 (2006).
[2] E. Dagotto, Science **309**, 257 (2005).
[3] A. P. Ramirez, in *Handbook of Magnetic Materials* Vol. 13, edited by K. J. H. Buschow (Elsevier Science, Amsterdam, 2001), p. 423.
[4] E. Dagotto and Y. Tokura, MRS Bull. **33**, 1037 (2008).
[5] H. Schmid, in *Introduction to Complex Mediums for Optics and Electromagnetics*, edited by W. S. Weiglhofer and A. Lakhtakia (SPIE Press, Bellingham, WA, 2003), p. 167.
[6] M. Fiebig, J. Phys. D **38**, R123 (2005).
[7] T. Kimura, T. Goto, H. Shintani, K. Ishizaka, T. Arima, and Y. Tokura, Nature (London) **426**, 55 (2003).
[8] H. Katsura, N. Nagaosa, and A. V. Balatsky, Phys. Rev. Lett. **95**, 057205 (2005).
[9] M. Mostovoy, Phys. Rev. Lett. **96**, 067601 (2006).
[10] M. Kenzelmann, A. B. Harris, S. Jonas, C. Broholm, J. Schefer, S. B. Kim, C. L. Zhang, S.-W. Cheong, O. P. Vajk, and J. W. Lynn, Phys. Rev. Lett. **95**, 087206 (2005).
[11] S. Dong, R. Yu, S. Yunoki, J.-M. Liu, and E. Dagotto, Phys. Rev. B **78**, 155121 (2008).
[12] M. Mochizuki and N. Furukawa, Phys. Rev. B **80**, 134416 (2009).
[13] T. Kimura, S. Ishihara, H. Shintani, T. Arima, K. T. Takahashi, K. Ishizaka, and Y. Tokura, Phys. Rev. B **68**, 060403(R) (2003).
[14] J. Hemberger, F. Schrettle, A. Pimenov, P. Lunkenheimer, V. Yu. Ivanov, A. A. Mukhin, A. M. Balbashov, and A. Loidl, Phys. Rev. B **75**, 035118 (2007).
[15] Y. Yamasaki, S. Miyasaka, T. Goto, H. Sagayama, T. Arima, and Y. Tokura, Phys. Rev. B **76**, 184418 (2007).
[16] T. Goto, T. Kimura, G. Lawes, A. P. Ramirez, and Y. Tokura, Phys. Rev. Lett. **92**, 257201 (2004).
[17] The total angular momentum is zero in $Eu^{3+}$ with $4f^6$ configuration and $Y^{3+}$ is nonmagnetic. Thus, only Mn moment can contribute the weak ferromagnetism in $Eu_{1-x}Y_xMnO_3$.
[18] J. Agostinho Moreira, A. Almeida, W. S. Ferreira, M. R. Chaves, S. M. F. Vilela, and P. B. Tavares, arXiv:0903.5471 (unpublished).
[19] Contribution of the $T$ dependence of gauge resistance to the $\Delta L(T)/L$ data was not completely subtracted, which may cause a more pronounced low-temperature upturn in the $\Delta L(T)/L$-$T$ curves than those in the lattice-parameter data.
[20] I. Solovyev, N. Hamada, and K. Terakura, Phys. Rev. Lett. **76**, 4825 (1996).
[21] V. Skumryev, F. Ott, J. M. D. Coey, A. Anane, J.-P. Renard, L. Pinsard-Gaudart, and A. Revcolevschi, Eur. Phys. J. B **11**, 401 (1999).
[22] An electric field of $\sim$0.3 MV/m was always applied during the measurements shown in Fig. 2(b). We confirmed that no finite polarization was observed along $b$ and $c$ in the present experimental condition.